

# Numerical Comparisons of Three Recently Proposed Algorithms in the Protein Folding Problem

ULRICH H. E. HANSMANN,<sup>1,2</sup> YUKO OKAMOTO<sup>2</sup>

<sup>1</sup>Swiss Center for Scientific Computing (SCSC)

Eidgenössische Technische Hochschule (ETH) Zürich, 8092 Zürich, Switzerland

<sup>2</sup>Department of Theoretical Studies, Institute for Molecular Science (IMS), Okazaki, Aichi 444, Japan

Received 8 July 1996, accepted 30 September 1996

**ABSTRACT:** We numerically compare the effectiveness of three recently proposed algorithms, multicanonical algorithm, simulations in a  $1/k$ -sampling, and simulated tempering, for the protein folding problem. We perform simulations with high statistics for one of the simplest peptides, met-enkephalin. While the performances of all three approaches is much better than traditional methods, we find that the differences among the three are only marginal.

© 1997 by John Wiley & Sons, Inc. *J Comput Chem* 18: 920–933, 1997

**Keywords:** Monte Carlo; generalized ensemble; protein folding; multiple-minima problem; global energy minimization

## Introduction

While there has been considerable progress in numerical simulations of biological macromolecules over the last 30 years (for a recent

review see, for example, ref. 1), the prediction of their low-energy conformations from the first principles remains a formidable task. The numerical calculation of physical quantities depends on how comprehensively the phase space of the system is explored. However, the energy landscape of the system of peptides and proteins is characterized by a multitude of local minima separated by high energy barriers. At low temperatures, traditional Monte Carlo and molecular dynamics simulations tend to get trapped in one of these local minima. Hence, only small parts of the phase space are sampled (in a finite number of simulation steps) and physical quantities cannot be calculated accurately. A common approach to alleviate this multiple-minima problem is to identify the global mini-

Correspondence to: V. H. E. Hansmann or Y. Okamoto; e-mail: hansmann@ims.ac.jp or okamotoy@ims.ac.jp

Contract grant sponsor: Department of Energy, contract grant number: DE-FC05-85ER2500

Contract grant sponsor: Schweizerische NationalFonds, contract grant number: 20-40838.94

Contract grant sponsor: Japanese Ministry of Education, Science, Sports and Culture

Contract grant sponsor: Japan Society for the Promotion of Science

mum in the *free* energy (which should correspond to the native conformation of a protein) with the lowest potential energy conformation, ignoring entropic contributions, and to search for this conformation with powerful optimization techniques such as Monte Carlo with minimization,<sup>2</sup> genetic algorithms,<sup>3</sup> or simulated annealing.<sup>4</sup> Since simulated annealing was first introduced to the protein folding problem,<sup>5–8</sup> the effectiveness was tested with many peptides and proteins, and it is now one of the most popular optimization methods used in the field (for a recent review see Ref. 9).

It is claimed that a variety of recently proposed methods like the *multicanonical approach*,<sup>10,11</sup> *entropic sampling*,<sup>12</sup> *simulated tempering*,<sup>13,14</sup> and simulations in a so-called *1 / k-ensemble*<sup>15</sup> allow a much better sampling of the phase space than previous methods. Actually, two of these methods, the multicanonical approach and entropic sampling, are mathematically identical as shown in ref. 16. The multicanonical algorithm was first applied to the protein folding problem in ref. 17. In ref. 18 the investigators showed that this new ansatz indeed leads to an improvement over simulated annealing. The method was also applied to the studies of the coil-globule transitions of a model protein<sup>19</sup> and the helix-coil transitions of homooligomers of nonpolar amino acids.<sup>20</sup> Simulated tempering was applied to the study of a model heteropolymer.<sup>21</sup>

Applications of simulated tempering and the *1 / k-ensemble* to protein folding problems are not yet available. Also not available is a quantitative comparison of the effectiveness of these three new methods. In the present article we try to fill in this gap. By simulating one of the simplest peptides, met-enkephalin, with high statistics, we study the numerical performances of the three methods. In particular, the efficiency of finding the global-minimum-energy conformation and calculating thermodynamic quantities is studied in detail.

## Methods

### ALGORITHMS

Although the algorithms are explained in the original studies, we briefly summarize here the ideas and implementations of the three approaches for completeness.

Simulations in the canonical ensemble weight each configuration with the Boltzmann factor,  $w_B(T, E) = e^{-\beta E}$ , and yield the usual bell-shaped

probability distribution of energy at temperature  $T$ :

$$P_B(T, E) \propto n(E)w_B(T, E) = n(E)e^{-\beta E} \quad (1)$$

where  $n(E)$  is the density of states (spectral density) and  $\beta = 1/k_B T$  is the inverse temperature (we set the Boltzmann constant,  $k_B$ , to unity hereafter).

Using local updates, the probability for the system to cross an energy barrier is proportional to  $e^{-\beta \Delta E}$  in the canonical ensemble. Here,  $\Delta E$  is the height of the energy barrier. Hence, at low temperatures (large  $\beta$ ), simulations will easily get trapped in one of the local minima and very long simulations are necessary to calculate thermodynamic quantities accurately. In general, one can think of two strategies to alleviate this problem. First, one can look for an improved updating scheme. For instance, a kind of *global* updating scheme called the cluster update method<sup>22,23</sup> is popular in spin systems. No such global updates are known for proteins. Second, one can perform the simulation in a “generalized ensemble,” where the above difficulty does not arise. The latter approach is the one that is investigated in the present article.

In the multicanonical approach<sup>10,11</sup> configurations with energy  $E$  are updated with a weight:

$$w_{mu}(E) \propto \frac{1}{n(E)} = e^{-S(E)} \quad (2)$$

where:

$$S(E) = \log n(E) \quad (3)$$

is the microcanonical entropy. A simulation with this weight factor will produce a uniform distribution of energy:

$$P_{mu}(E) \propto n(E)w_{mu}(E) = \text{const} \quad (4)$$

resulting in a free random walk in the energy space. This allows the simulation to escape from any energy barrier, and even regions with small  $n(E)$  can be explored in detail.

Unlike in a canonical simulation the weight,  $w_{mu}(E)$ , is not known *a priori* [in fact, the knowledge of the exact weight is equivalent to obtaining the density of states  $n(E)$ , i.e., solving the system], and one needs its estimator for a numerical simulation. Hence, the multicanonical ansatz consists of three steps: In the first step the estimator of the multicanonical weight factor  $w_{mu}(E)$  is calculated. Then one performs with this weight a multicanonical simulation with high statistics. In this way

information is collected over the whole energy range. We note that there is no explicit temperature dependence in simulations of the multicanonical ensemble. However, from this simulation one cannot only locate the energy global minimum but also obtain the canonical distribution at any inverse temperature,  $\beta = 1/T$ , for a wide range of temperatures using the reweighting techniques:<sup>24</sup>

$$P_B(T, E) \propto P_{mu}(E) w_{mu}^{-1}(E) e^{-\beta E} \quad (5)$$

This allows one to calculate the expectation value of any physical quantity,  $\mathcal{O}$ , at temperature  $T$  by:

$$\langle \mathcal{O} \rangle_T = \frac{\int dE \mathcal{O}(E) P_B(T, E)}{\int dE P_B(T, E)} \quad (6)$$

The crucial step is the calculation of the estimator for the multicanonical weight factor,  $w_{mu}(E)$ . It is obtained by an iterative procedure. The improved estimator of the multicanonical weight for the  $i$ th iteration is calculated from the histogram of energy distribution,  $P_{mu}^{(i-1)}(E)$ , and the weight  $w_{mu}^{(i-1)}$  of the preceding simulation as follows:

$$w_{mu}^{(i)}(E) = \frac{w_{mu}^{(i-1)}(E)}{P_{mu}^{(i-1)}(E)} \quad (7)$$

The first iteration is a canonical simulation at sufficiently high temperature,  $T_0 = 1/\beta_0$ , with  $w_{mu}^{(1)}(E) = e^{-\beta_0 E}$ . For details, see Refs. 18 and 20. The method for calculating the multicanonical weight factor is by no means unique. Although it is quite general, it has the disadvantage that it requires iterations of short simulations, the number of which is not known *a priori*.

Performing simulations in a so-called  $1/k$ -ensemble is a way of sampling the (microcanonical) entropy  $S$  uniformly:

$$P_{1/k}(S) = \text{const} \quad (8)$$

This equation implies that:

$$P_{1/k}(E) = P_{1/k}(S) \frac{dS}{dE} \propto \frac{dS}{dE} = \tilde{\beta}(E) \quad (9)$$

where  $\tilde{\beta}(E)$  stands for the *effective* inverse temperature,\* and is defined by:

$$\tilde{\beta}(E) \equiv \frac{1}{\tilde{T}(E)} = \frac{d \log n(E)}{dE} \quad (10)$$

There is again no explicit temperature dependence in simulations of the  $1/k$ -ensemble; it can be said

that simulations in both multicanonical and  $1/k$ -ensembles include information of *all* temperatures. If the simulation is restricted to a certain energy interval, eq. (10) defines the corresponding temperature range [assuming  $n(E)$  is a monotonous function of  $E$ ] over which reliable results can be obtained.

In their original article, Hesselbo and Stinchcombe<sup>15</sup> proposed that configurations are assigned a weight:

$$w_{1/k}(E) \propto \frac{1}{k(E)} \quad (11)$$

where the function,  $k(E)$ , is defined as the integral of density of states with respect to energy  $E$ :

$$k(E) = \int_{-\infty}^E dE' n(E') \quad (12)$$

This implies that:

$$P_{1/k}(E) \equiv n(E) w_{1/k}(E) = \frac{n(E)}{k(E)} = \frac{d \log k(E)}{dE} \quad (13)$$

Because the density of states  $n(E)$  is a rapidly increasing function of energy, we have  $\log k(E) \approx \log n(E)$  for wide range of values of  $E$ . Hence, eqs. (9) and (13) are equivalent, and a random walk in the entropy space is realized. Because the entropy  $S(E)$  is a monotonically increasing function of energy, a random walk in entropy implies a random walk in energy space [with more weight toward low-energy region; compare eqs. (2) and (11)]. Hence, a simulation in the  $1/k$ -ensemble can escape from any energy barrier. Hesselbo and Stinchcombe claim that the  $1/k$ -sampling is superior to the multicanonical algorithm in the sense that less sampling is necessary for the former.<sup>15</sup>

In numerical work, energy is discretized and integrals are replaced by sums. Again, the weight,  $w_{1/k}(E)$ , is not known *a priori* and its estimator has to be calculated. It is obvious that the method just described for determination of the multicanonical weight factor is also suited for the calculation of weight in the  $1/k$ -ensemble. In addition, it follows from the definitions of the weights, eqs. (2), (11), and (12), that one can calculate  $w_{1/k}(E)$  from  $w_{mu}(E)$ , and *vice versa*. Thermodynamic quantities at any temperature can be calculated by eq. (6)

\*We remark that the term "multicanonical algorithm" was inspired by this effective temperature. In early work, Berg and coworkers used, for the multicanonical weight, the specific parameterization  $\exp(-\tilde{\beta}(E)E - \alpha(E))$ , approximating  $S(E) = \log n(E)$  by straight lines between adjacent energy bins.

with the reweighting techniques of eq. (5), in which  $P_{mu}(E)$  and  $w_{mu}(E)$  are replaced by  $P_{1/k}(E)$  and  $w_{1/k}(E)$ , respectively.

The third approach is simulated tempering, which was first introduced under the name *method of expanded ensembles* by Luyabartsev et al.,<sup>13</sup> but became more popular under the former name proposed by Marinari and Parisi in ref. 14. In this approach, temperature itself becomes a dynamic variable. Temperature and configuration are both updated with a weight:

$$w_{ST}(T, E) \propto e^{-E/T - g(T)} \quad (14)$$

where the function,  $g(T)$ , is chosen so that the probability distribution of temperature is given by:

$$P_{ST}(T) = \int dE n(E) e^{-E/T - g(T)} = \text{const} \quad (15)$$

Hence, in simulated tempering, the *temperature* is sampled uniformly, while simulations in multicanonical and  $1/k$ -ensembles respectively sample energy and entropy uniformly. A random walk in temperature space is realized, allowing the simulation to escape from any energy barrier. The last equation, eq. (15), implies that:

$$e^{g(T)} \propto \int dE n(E) e^{-E/T} \quad (16)$$

The function,  $g(T)$ , is therefore proportional to the logarithm of the canonical partition function at temperature  $T$ . Again, the weight,  $w_{ST}(T, E)$ , is not known *a priori*, and its estimator has to be calculated. We remark, however, that eq. (16) easily allows calculation of the function  $g(T)$ , and therefore of the weight,  $w_{ST}(T, E)$ , once the multicanonical weight,  $w_{mu}(E) = n^{-1}(E)$ , is given. Likewise, the multicanonical weight,  $w_{mu}(E)$ , can in principle be calculated from  $g(T)$  by the inverse Laplace transformation.

In the numerical work the temperature is discretized and restricted to a certain interval  $[T_{min}, T_{max}]$ . Integrals are replaced by sums. We also found it convenient to choose the temperature points,  $T_i$ , not equidistant, but so that the increment of adjacent temperature points decreases exponentially with decreasing temperature. Of course, this implies that we do not sample in a uniform way in temperature, but rather by a monotone function of temperature.

Given parameters  $g_i = g(T_i)$  a simulated tempering simulation may use the conventional Metropolis algorithm [25] with two kinds of Monte

Carlo updates:

- Updates of configurations (conformations) at a fixed temperature,  $T_i$ , with probability  $\min\{1, \exp[-(E_{new} - E_{old})/T_n]\}$ .
- Updates of temperatures with a fixed configuration (conformation) with probability  $\min\{1, \exp[-E(1/T_{new} - 1/T_{old}) - (g(T_{new}) - g(T_{old}))]\}$ .

Using these updates, one can perform a simulated tempering simulation.

Crucial for this method is again the determination of the parameters  $g_i$  ( $i = 1, \dots, n$ ). Given the temperature points,  $T_i$  ( $i = 1, \dots, n$  with  $T_1 = T_{max} \geq T_i \geq T_n = T_{min}$ ),  $g_i$  can be calculated by the following iterative procedure:

1. Start with a short canonical simulation of  $m_1$  MC sweeps, updating only configurations at temperature  $T_1 = T_{max}$ , and calculate the average energy,  $\langle E \rangle_{T_1}$ . Formally, this can be regarded as a simulated tempering simulation at a fixed temperature,  $T_1$ , with weight  $w_{ST}(T, E) = e^{-E/T_1 - g_1}$  and  $g_1 = 0$ .
2. Calculate new parameters  $g_j$  according to:

$$g_j = \begin{cases} g_j + \log(m_j), & 1 \leq j \leq i \\ g_j + \langle E \rangle_{T_i} \left( \frac{1}{T_{i+1}} - \frac{1}{T_i} \right), & j = i + 1 \\ \infty, & j > i + 1 \end{cases} \quad (17)$$

3. Start a new simulation, now updating both configurations and temperatures, with weight  $w_{ST}(T, E) = e^{-E/T_j - g_j}$ , and sample the distribution of temperatures  $T_j$  in the histogram  $m_j = m(T_j)$ . For  $T = T_{i+1}$  calculate the average energy  $\langle E \rangle_{T_{i+1}}$ .
4. If the histogram  $m_j$  is approximately flat in the temperature range  $T_1 \geq T_j \geq T_{i+1}$ , set  $i = i + 1$ . Otherwise, leave  $i$  unchanged.
5. Iterate the last three steps until the obtained temperature distribution,  $m_j$ , becomes flat over the whole temperature range  $[T_n = T_{min}, T_1 = T_{max}]$ .

Once the weight factor,  $w_{ST}(T, E)$ , is obtained, we make a production run with high statistics. Physical quantities have to be sampled for each temperature point separately. Their expectation values at temperature  $T$  are then calculated in the

usual way by:

$$\langle \mathcal{O} \rangle_T = \frac{\int dx \mathcal{O}(x) e^{-E(x)/T}}{\int dx e^{-E(x)/T}} \quad (18)$$

where  $x$  labels the conformations, and only those conformations that were obtained at temperature  $T$  are included in the integral. Expectation values at intermediate temperatures can be calculated by the reweighting techniques.<sup>24</sup>

## PEPTIDE PREPARATION AND POTENTIAL ENERGY FUNCTION

Met-enkephalin has the amino-acid sequence Tyr-Gly-Gly-Phe-Met. For our simulations the backbone was terminated by a neutral  $\text{NH}_2$ -group at the N-terminus and a neutral  $-\text{COOH}$  group at the C-terminus as in previous works with met-enkephalin.<sup>2,7,17,26,27</sup> The potential energy function,  $E_{\text{tot}}$ , that we used is given by the sum of the electrostatic term,  $E_{\text{es}}$ , the 12-6 Lennard-Jones term,  $E_{\text{vdW}}$ , and the hydrogen-bond term,  $E_{\text{hb}}$ , for all pairs of atoms in the peptide together with the torsion term,  $E_{\text{tors}}$ , for all torsion angles:

$$E_{\text{tot}} = E_{\text{es}} + E_{\text{vdW}} + E_{\text{hb}} + E_{\text{tors}} \quad (19)$$

$$E_{\text{es}} = \sum_{(i,j)} \frac{332 q_i q_j}{\epsilon r_{ij}}, \quad (20)$$

$$E_{\text{vdW}} = \sum_{(i,j)} \left( \frac{A_{ij}}{r_{ij}^{12}} - \frac{B_{ij}}{r_{ij}^6} \right) \quad (21)$$

$$E_{\text{hb}} = \sum_{(i,j)} \left( \frac{C_{ij}}{r_{ij}^{12}} - \frac{D_{ij}}{r_{ij}^{10}} \right) \quad (22)$$

$$E_{\text{tors}} = \sum_l U_l (1 \pm \cos(n_l \chi_l)) \quad (23)$$

where  $r_{ij}$  is the distance between the atoms  $i$  and  $j$ , and  $\chi_l$  is the  $l$ th torsion angle. This  $E_{\text{tot}}$  was used in the actual simulations of the three algorithms. The parameters ( $q_i$ ,  $A_{ij}$ ,  $B_{ij}$ ,  $C_{ij}$ ,  $D_{ij}$ ,  $U_l$ , and  $n_l$ ) for the energy function were adopted from ECEPP/2.<sup>28-30</sup> The computer code, KONF90,<sup>31</sup> was used. The peptide-bond dihedral angles  $\omega$  were fixed at the value  $180^\circ$  for simplicity, which leaves 19 angles  $\phi_i$ ,  $\psi_i$ , and  $\chi_i$  as independent variables. We remark that KONF90 uses a different convention for the implementation of the ECEPP parameters. Therefore, our energy values are slightly different from those of the original implementation of ECEPP/2.

## COMPUTATIONAL DETAILS

Preliminary runs showed that all methods needed roughly the same amount of CPU time for a fixed number of MC sweeps (about 15 minutes for 10,000 sweeps on an IBM-RS6000 320H). Hence, we compared the different methods by performing simulations with the same number of total MC sweeps. By setting this number to 1,000,000 sweeps we tried to ensure high statistics. One MC sweep updates every torsion angle of the peptide once.

In the case of simulated tempering we chose 30 temperature points that were exponentially distributed between  $T_{\text{min}} = 50$  K and  $T_{\text{max}} = 1000$  K; that is,  $T_i = T_{\text{max}} \times \gamma^{(i-1)}$  ( $i = 1, \dots, 30$ ) with  $\gamma = (T_{\text{min}}/T_{\text{max}})^{1/29}$ . This specific choice of temperature points was made because we found in preliminary runs that, for an equidistant distribution of temperatures, we either needed a very large number of intermediate temperature points or we could not obtain reliable estimates for  $g_i = g(T_i)$ . Even with the aforementioned choice of temperature points we needed 150,000 sweeps to calculate the simulated tempering parameters  $g_i$ .

In our earlier work<sup>17</sup> we found that we needed 40,000 sweeps to calculate the multicanonical weight for met-enkephalin. To better compare the different methods we tried to improve the weights by further iterations until the total number of sweeps was again 150,000. Although the weight for the  $1/k$ -ensemble can also be determined by the iterative procedure, here we just calculated it from the obtained multicanonical weight by means of eq. (12) to save computation time.

All thermodynamic quantities were then calculated from a production run of 1,000,000 MC sweeps for each of the three methods which followed 10,000 sweeps for thermalization. At the end of every second sweep we stored the energy of the actual conformation for future analysis of thermodynamic quantities. In all cases, the simulations started from completely random initial conformations ("hot start").

## Results and Discussion

We start this section by demonstrating some of the basic features of the three methods. As explained earlier, we expect for all three algorithms that simulations result in a (weighted) random walk in energy space. In Figure 1 we show the time series of energy from the production runs of 1,000,000 MC sweeps for the three methods. They

all exhibit a random walk between low energy states and high energy states. In ref. 27 it was shown that, with the energy parameters of KONF90, conformations with potential energies less than  $-11$  kcal/mol essentially have the same structure (with small deviations in dihedral angles), which is conformation with the global-minimum energy. The random walks in Figure 1 all reached this lowest energy state many times. The numbers of such independent visits are examined in what follows.

By comparing eqs. (2) and (11), one expects that the random walk in the  $1/k$ -ensemble is supposed to be biased toward the low-energy region, whereas that in the multicanonical ensemble does not have any bias (free random walk). This tendency is apparent in the random walks in Figure 1; that of the  $1/k$ -ensemble spends more time in the low-energy region.

In Figure 2 histograms of energy distribution for the three methods are shown. As expected, the distribution is essentially flat for the multicanonical ensemble; it increases with decreasing energy for the  $1/k$ -ensemble. As implied by eq. (9),  $P_{1/k}(E) \times \tilde{T}(E)$  is a flat curve (data not shown). Here,  $\tilde{T}(E)$  is the effective temperature defined in eq. (10). The distribution of energies for simulated tempering given in Figure 2 is also flat, but has the tendency to increase as energy decreases. The flat distribution does not imply uniform sampling of temperature, because our temperature points are not equidistant. For equidistant temperature points we would expect a distribution proportional to the reciprocal of the specific heat.

In the  $1/k$ -ensemble a free random walk in entropy space is expected to be realized [see eq. (8)]. In Figure 3a the time series of the function  $S(E) = \log n(E)$  is shown. A random walk between small  $S$  and large  $S$  is indeed observed. In Figure 3b we display the probability distribution of entropy for both simulations of multicanonical and  $1/k$  ensembles. This should be compared with Figure 2, where we displayed histograms of energy distribution. The multicanonical simulation yields a curve which increases with entropy, whereas in the  $1/k$  ensemble we observe a flat distribution, indicating that entropy was indeed uniformly sampled.

In simulated tempering the weight is chosen so that a one-dimensional random walk in temperature points  $T_i$  is obtained [see eq. (15)]. This can be seen in Figure 4, where we display the time series of temperature for simulated tempering. As expected, a random walk between high and low

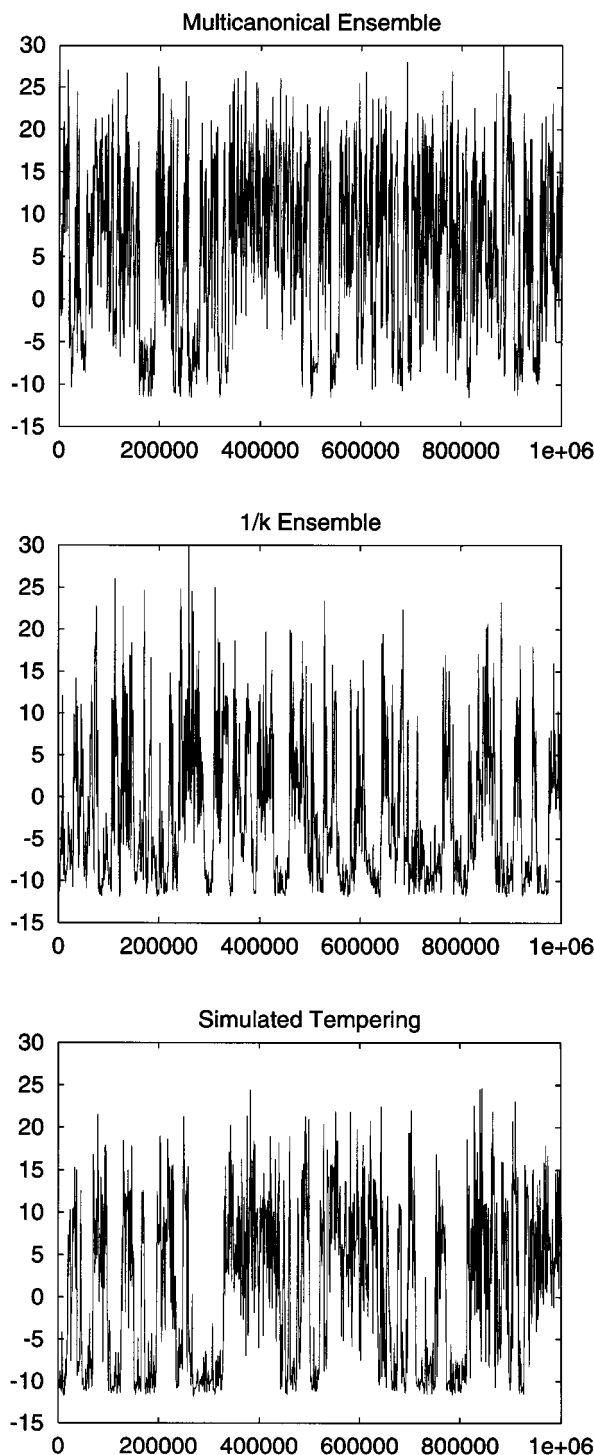


**FIGURE 1.** Time series of energy,  $E$  (kcal / mol), from a simulation of 1,000,000 MC sweeps by multicanonical,  $1/k$ -sampling, and simulated tempering algorithms.

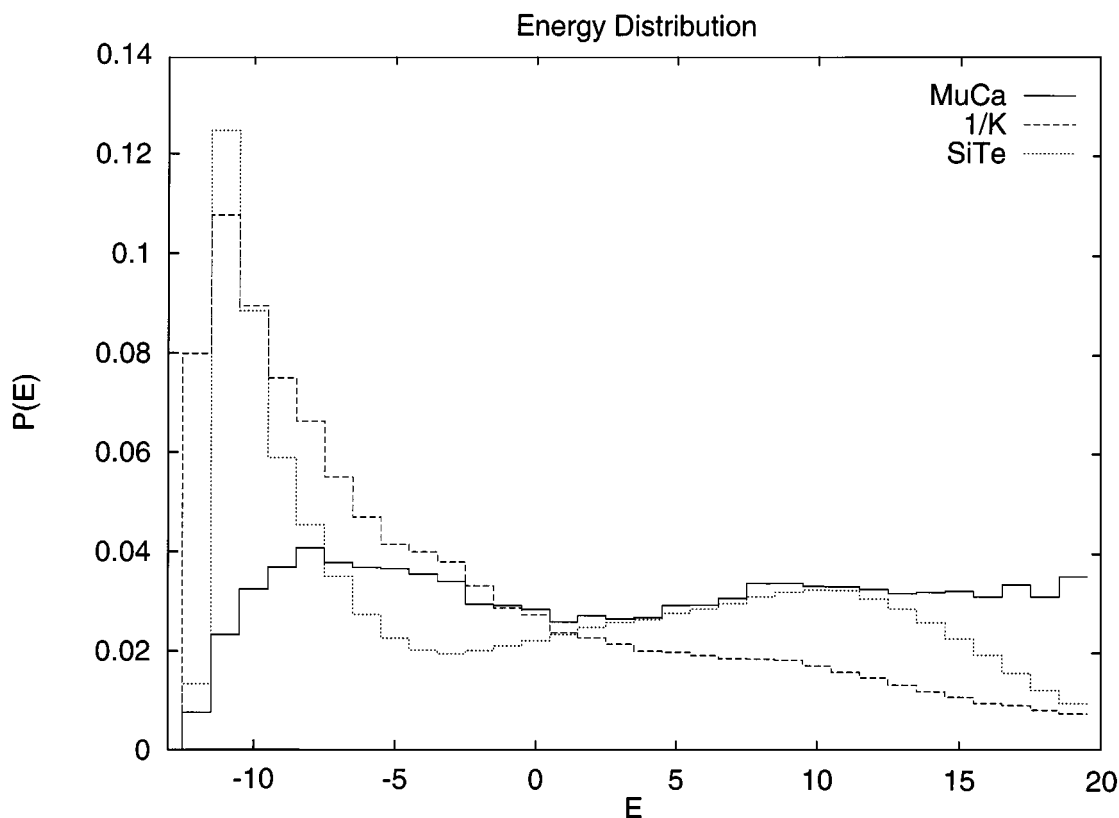


**FIGURE 2.** Probability distribution of energy,  $E$  (kcal/mol), from simulations by the three methods. The data rely on 1,000,000 MC sweeps for each simulation.

temperatures is observed. Because all temperatures should appear with the same weight, we expect that the distribution of temperatures is essentially flat. The simulation results confirmed this within the deviations of factor 2 from flatness (data not shown). As in the case of the multicanonical approach, one must make a trade-off between the numerical effort one is willing to put into determination of weights and the deviation from a flat probability distribution one is willing to accept. We allowed for differences of less than one order of magnitude.

A major advantage of all three methods studied in this article is that they allow calculations of thermodynamics quantities at any temperature from just one simulation run, once the weights are determined [see eqs. (6) and (18)]. For example, in Figure 5 we show the average potential energy,  $\langle E \rangle_T$ , and the specific heat,  $C$ , as functions of temperature. The latter quantity is defined by:

$$C(T) = \beta^2 \frac{\langle E^2 \rangle_T - \langle E \rangle_T^2}{N} \quad (24)$$

where  $N (= 5)$  is the number of amino acids in the peptide. All three methods yield the same values at most of the temperature values within the (small) error bars. These results demonstrate that the three methods are equally well suited for calculation of thermodynamic quantities. They also prove that our estimates of these quantities are reliable (because they were calculated from independent simulation data obtained by different methods, and there is no systematic hidden bias). This is especially important for the low temperature region where comparison with canonical simulation is not possible. Note that the average potential energy at the lowest temperature region is about  $-12$  kcal/mol, which is the global-minimum energy value for the energy function in KONF90.<sup>27</sup> The value at a high temperature, say  $T = 1000$  K, is as large as  $\approx 16$  kcal/mol. The energy fluctuation,  $\delta E$ , at this temperature is about 5 kcal/mol [calculated from the value of  $C$  from eq. (24) by  $\delta E = \sqrt{5C/\beta^2}$ ]. Hence, the random walks in Figure 1 have reached the high energy region with energy values that would be obtained at temperatures higher than 1000 K.

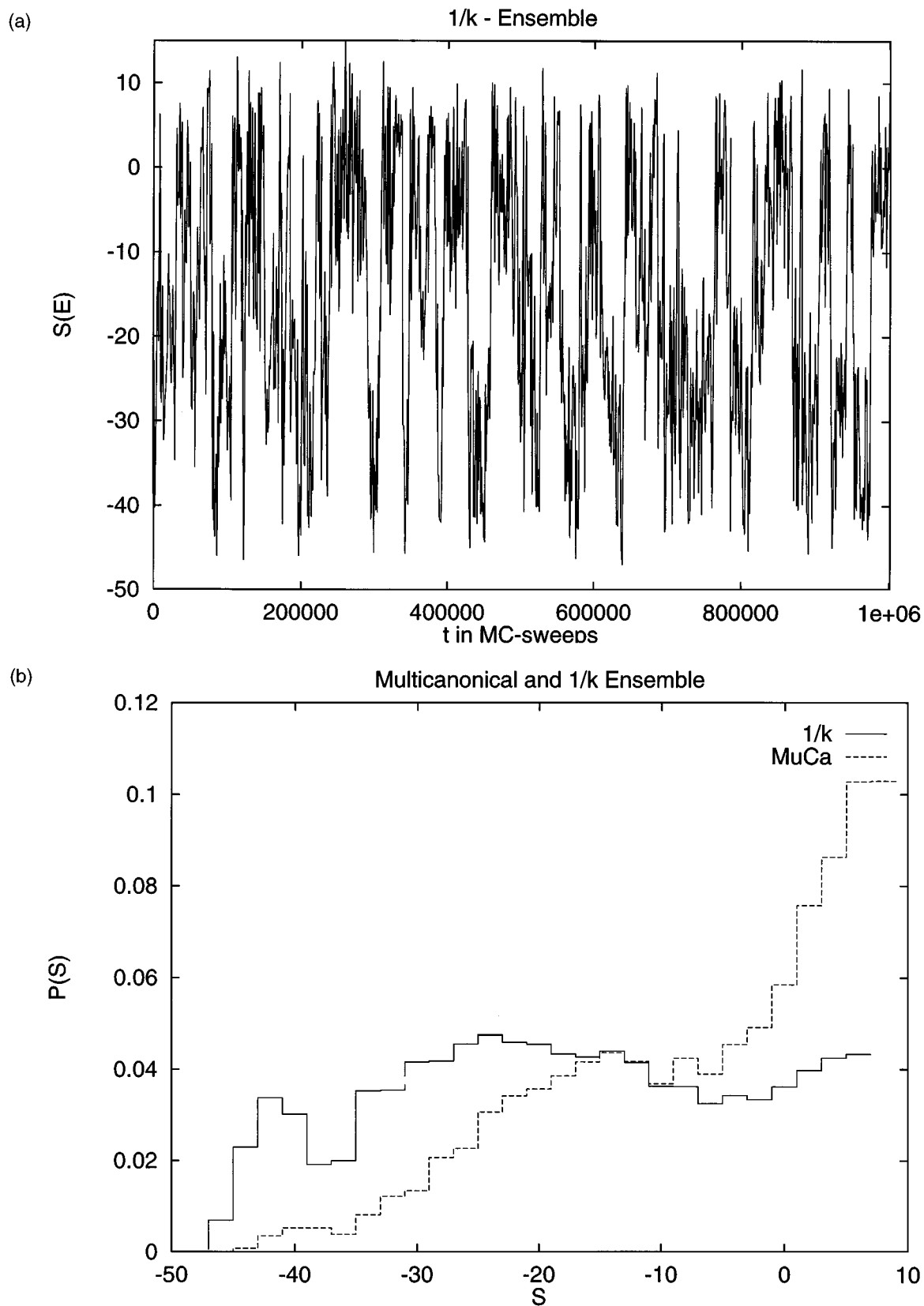


**FIGURE 3.** (a) Time series of entropy,  $S$ , from a  $1/k$ -ensemble simulation of 1,000,000 MC sweeps. (b) Probability distribution of entropy,  $S$ , from simulations in multicanonical and  $1/k$  ensembles. The data rely on 1,000,000 MC sweeps for each simulation.



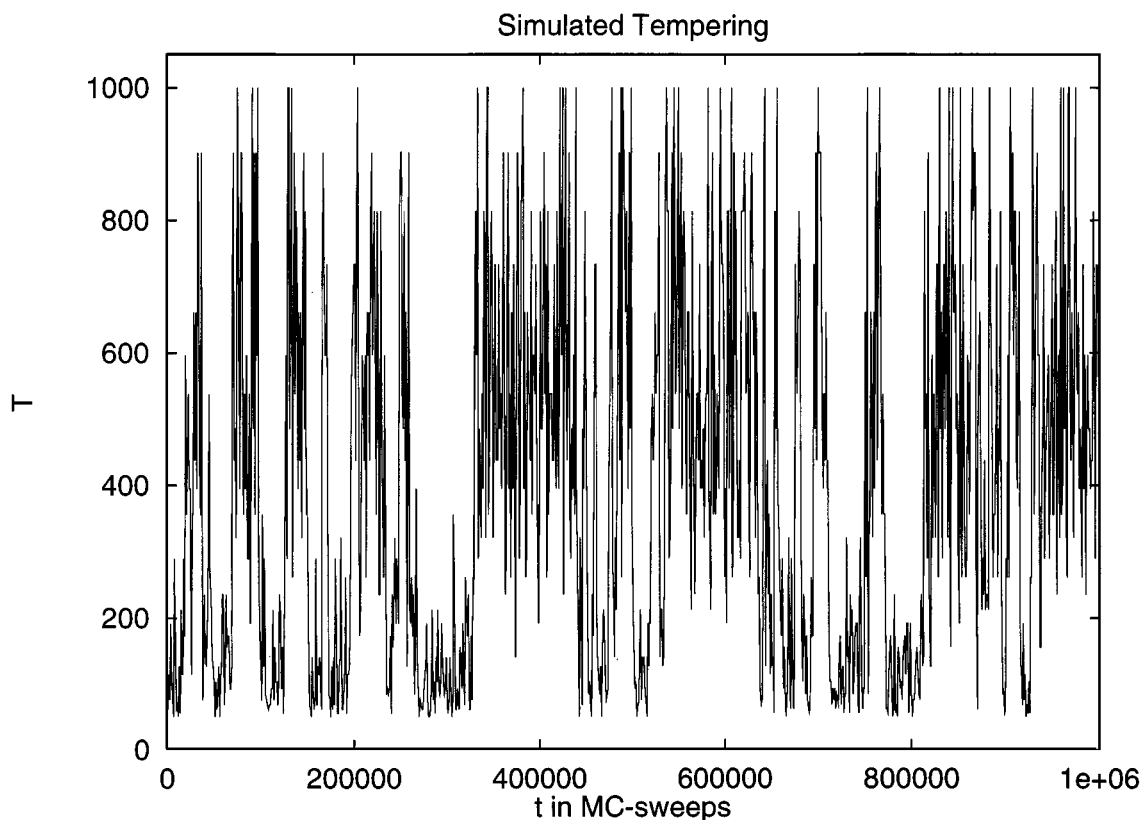


**FIGURE 4.** Time series of temperature,  $T$  (K), from a simulated tempering simulation of 1,000,000 MC sweeps.

The behavior of the specific heat is also reasonable. The peak at  $T \approx 300$  K implies that this temperature is most relevant for the folding of the peptide. The zero-temperature limit of the specific heat agrees with that of the harmonic approximation to the potential energy, where the equipartition theorem can be used:

$$\langle E \rangle = N_F \frac{T}{2} \quad (25)$$

Here,  $N_F$  is the number of degrees of freedom (number of torsion angles) and we have again set  $k_B = 1$ . The above specific heat is defined to be the derivative of average energy per residue with respect to temperature:

$$C = \frac{d(\langle E \rangle / N)}{dT} = \frac{N_F}{2N} \quad (26)$$

For met-enkephalin  $N_F = 19$  (number of free torsion angles) and  $N = 5$ , and we have  $C = 1.9$ . The zero-temperature limit extrapolated in Figure 5 agrees with this value.

A comparison of Figures 1 and 4 gives us a way of comparing the performance of the three methods in terms of sampling the ground-state conformations. It is evident that low energy (temperature) states, which are separated in the time series by high energy (temperature) states, are uncorrelated. The number of such "tunneling" events is therefore a lower limit for the number of independent low-energy states visited in the simulation. We define a tunneling event as the walk in the simulation between a conformation with energy,  $E \leq -11.0$  kcal/mol (i.e., a ground-state conformation) (or  $T = 50$  K in the case of simulated tempering), to a conformation with energy above  $E = 20.0$  kcal/mol (or  $T = 1000$  K for simulated tempering) and back to the ground-state region. For each tunneling event the lowest energy,  $E_{GS}$ , obtained during the corresponding cycle, was monitored. Table I summarizes our results. In our production runs of each of the 1,000,000 MC sweeps we observed 23 tunneling events for the multi-canonical simulation, 27 for the simulation in the  $1/k$ -ensemble, and 19 in the case of simulated tempering. These numbers correspond to tunneling times (average number of MC sweeps needed

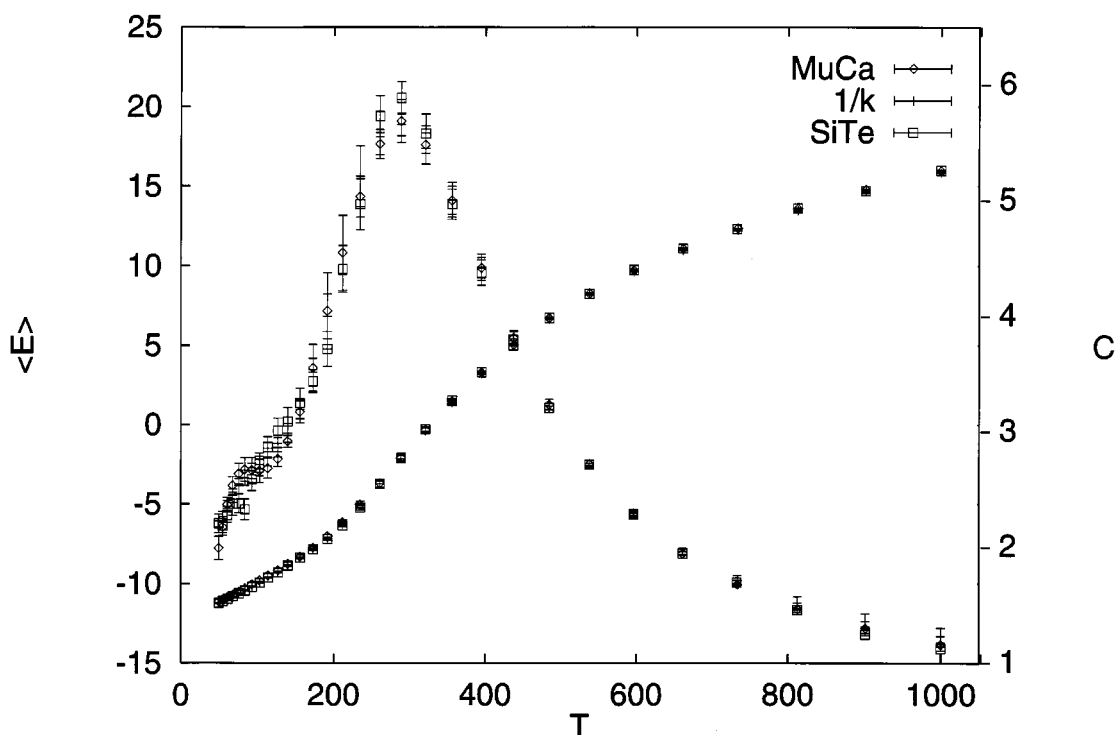


**FIGURE 5.** Average energy,  $\langle E \rangle_T$  (kilocalories per mole), and specific heat,  $C$ , as a function of temperature,  $T$  (K), calculated from the simulations of multicanonical ensemble,  $1/k$ -ensemble, and simulated tempering. The data rely on 1,000,000 MC sweeps for each method. The energy scale is displayed on the ordinate on the left-hand side and the specific heat on the right-hand side. The average energy is a monotonically increasing function of temperature, whereas the specific heat has a maximum around 300 K.

for a tunneling event) of 40,324, 35,664, and 47,874 MC sweeps for multicanonical,  $1/k$ -ensemble, and simulated tempering simulations, respectively. Note that the number of tunneling events from the multicanonical simulation is higher than the one quoted in ref. 18, where we found only 18 tunneling events and a tunneling time of 54,136. We assume that this improvement is due to the improvement of the multicanonical weight. It is interesting to observe that the number of tunneling events (and therefore independent ground-state conformations found in the course of simulation) is larger for the  $1/k$ -ensemble than for the multicanonical simulation. The observed differences may be due to large statistical fluctuations (see the standard deviations of tunneling times in the last row of Table I). In any case the differences in tunneling times that we found are too small to establish a ranking of the performances among the three methods.

We conclude that all three methods, while not differing much from each other, are much more efficient in finding independent ground-state

structures than traditional methods. In ref. 18 we made a comparison of multicanonical algorithms with simulated annealing, including annealing versions of the multicanonical simulations.<sup>32</sup> Multicanonical annealing simplifies the determination of weight factors and can be used to search ground states, but does not allow estimation of thermodynamic quantities. Here we also performed annealing simulations in  $1/k$ -ensemble and simulated tempering. Twenty independent annealing runs with 50,000 MC sweeps were made for the two methods. An annealing simulation in the  $1/k$ -ensemble was done in the same manner as for multicanonical annealing.<sup>18</sup> Namely, an upper bound in energy,  $E_{wall}$ , is introduced, above which a simulation is not allowed to enter. The weight is updated so that the energy distribution becomes flat in the interval  $(E_{wall} - \Delta E, E_{wall})$ , where  $\Delta E$ , the sampling energy interval, is a constant. The upper bound  $E_{wall}$  is lowered once after each iteration so that  $E_{wall} = E_0 + \Delta E$ , where  $E_0$  is the lowest energy found in the preceding iteration. A simulated tempering annealing simulation is im-

**TABLE I.**  
**Estimated Ground-State Energies,  $E_{GS}$  (in Kilocalories per Mole) of Each Tunneling Event As Obtained by the Three Algorithms.<sup>a</sup>**

$n_{tu}$	Multicanonical ensemble		1 / $k$ -ensemble		Simulated tempering	
	$t_{min}$	$E_{GS}$	$t_{min}$	$E_{GS}$	$t_{min}$	$E_{GS}$
0	24830	− 11.8	2162	− 11.8	12596	− 12.0
1	49472	− 11.7	29094	− 11.7	66286	− 11.8
2	160546	− 12.0	56382	− 12.0	106646	− 11.9
3	228340	− 11.9	85790	− 12.0	163430	− 12.0
4	240648	− 11.9	121798	− 12.0	183162	− 11.9
5	272908	− 11.8	168464	− 11.6	237592	− 11.7
6	294894	− 11.3	174704	− 11.8	273200	− 11.9
7	319722	− 12.1	209170	− 12.0	408646	− 11.3
8	330868	− 11.1	236218	− 11.9	446152	− 11.8
9	484056	− 11.7	299008	− 12.0	455142	− 11.8
10	503570	− 11.9	341488	− 12.1	465150	− 11.9
11	549780	− 11.7	389804	− 12.0	514524	− 11.8
12	623528	− 11.5	450304	− 12.1	639764	− 11.3
13	628398	− 11.8	500868	− 11.7	648672	− 11.4
14	651510	− 11.1	506178	− 11.9	665176	− 11.9
15	663014	− 11.5	516248	− 11.9	691068	− 11.8
16	681694	− 11.9	578230	− 12.0	746726	− 11.9
17	694916	− 11.3	588002	− 11.6	778272	− 12.0
18	815442	− 11.8	638984	− 12.0	899104	− 11.8
19	885534	− 11.1	691742	− 11.2	922208	− 11.8
20	911926	− 11.6	696882	− 11.9		
21	918322	− 11.7	705466	− 11.8		
22	949836	− 11.5	759824	− 11.9		
23	952284	− 11.2	803662	− 12.1		
24			875652	− 11.6		
25			890076	− 12.0		
26			922426	− 11.9		
27			965106	− 12.0		
$\langle t_{tun} \rangle$	40324(39826)		35664(19633)		47874(37777)	

<sup>a</sup> $t_{min}$  is the sweep when the simulation first entered the ground-state region ( $E \leq -11.0$  kcal/mol) in the corresponding tunneling event.  $\langle t_{tun} \rangle$  is the average time in Monte Carlo sweeps between these tunneling events. The numbers in brackets are the standard deviations of the corresponding quantities.

plemented similarly by replacing energy with temperature in the above procedure (for details of the annealing algorithms, see ref. 18).  
The lowest energies obtained by each annealing run are summarized for the three methods and compared with simulated annealing in Table II, where the values for multicanonical annealing and simulated annealing were taken from ref. 18. The results are similar with a high probability (75% to 90%) of finding the global minimum of energy in contrast to the moderate probability (around 40%) of those by Monte Carlo simulated annealing without much fine-tuning of the annealing schedule.<sup>18</sup> To compare different annealing schedules we varied the number of independent runs and MC

sweeps per run keeping their product constant. The results are shown in Table III, where data for multicanonical annealing and simulated annealing were taken from ref. [18]. Again, our results do not allow a ranking of the generalized ensemble algorithms, but show that they perform better than simulated annealing.  
To obtain an optimal annealing schedule, one has to monitor the specific heat. One has to lower the temperature very slowly where the specific heat has a peak so that a wide variety of conformations are sampled. From Figure 5 one finds that the present system of met-enkephalin has a peak of specific heat at  $\approx 300$  K. This temperature, in turn, corresponds to the average potential energy

**TABLE II.**  
**Lowest Energy (in Kilocalories per Mole) Obtained by the 20 Annealing Runs of the Three Algorithms.<sup>a</sup>**

Run	Multicanonical	1 / <i>k</i>	Simulated tempering	Simulated annealing
1	−11.6	−10.3	−11.8	−11.7
2	−12.0	−11.7	−11.7	−8.6
3	−10.2	−11.3	−11.5	−12.1
4	−10.1	−11.6	−11.4	−8.8
5	−11.9	−12.1	−11.1	−7.4
6	−12.0	−11.8	−11.1	−8.9
7	−11.9	−10.9	−11.6	−12.1
8	−11.7	−10.4	−11.5	−12.2
9	−11.8	−11.7	−11.4	−7.1
10	−11.9	−11.4	−11.5	−7.5
11	−12.0	−11.3	−11.3	−9.9
12	−12.1	−11.9	−10.5	−7.3
13	−12.0	−11.4	−12.0	−8.4
14	−11.8	−12.0	−9.0	−10.6
15	−11.3	−11.6	−11.8	−10.3
16	−11.9	−11.5	−10.9	−12.2
17	−12.0	−11.7	−11.4	−12.2
18	−11.9	−9.3	−10.7	−9.1
19	−11.9	−11.6	−11.1	−11.9
20	−11.6	−10.5	−11.7	−12.1
<i>n</i> <sub>GS</sub>	18 / 20	15 / 20	16 / 20	8 / 20

<sup>a</sup>For comparison, the results from simulated annealing are also included. For all cases, the total number of Monte Carlo sweeps per run was 50,000. *n*<sub>GS</sub> is the number of runs in which a conformation with  $E \leq -11.0$  kcal/mol was obtained. The data for multicanonical annealing and simulated annealing were taken from ref. 18.

of  $\approx -1$  kcal/mol, as shown in Figure 5. Because the lowest energy is about  $-12$  kcal/mol, we conclude that the sampling energy interval,  $\Delta E$ ,<sup>18</sup> for the annealing simulations in multicanonical and 1/*k*-ensembles should be more than 11 [−1 − (−12)] kcal/mol. The results in Table II were obtained with  $\Delta E = 15$  kcal/mol. As for the simulated tempering annealing simulation, we conclude that the corresponding sampling temperature interval,  $\Delta T$ , should be at least  $\Delta T = 250$  ( $300 - T_{min}$ ) K. The results in Table II were ob-

tained with  $\Delta T = 300$  K. These analyses give some hint to the determination of optimal annealing conditions.

Finally, in Figure 6 we show the time series of energy from typical annealing runs for the multicanonical algorithm, 1/*k*-ensemble, simulated tempering, and simulated annealing. From Figure 6 we can understand why the performances of the former three algorithms were better than a regular simulated annealing with naive exponential annealing schedule of ref. 31 (without reheating).

**TABLE III.**  
**Number of Runs that Reached Ground-State Conformations for the Three Algorithms.<sup>a</sup>**

Number of runs × number of MC sweeps	Multicanonical	1 / <i>k</i>	Simulated tempering	Simulated annealing
10 × 100,000	10	9	9	5
20 × 50,000	18	15	16	8
50 × 20,000	21	22	17	10
100 × 10,000	28	29	20	13

<sup>a</sup>Keeping the total number of MC sweeps constant we varied the number of independent runs. For comparison, simulated annealing data are included. The data for multicanonical annealing and simulated annealing were taken from ref. 18.

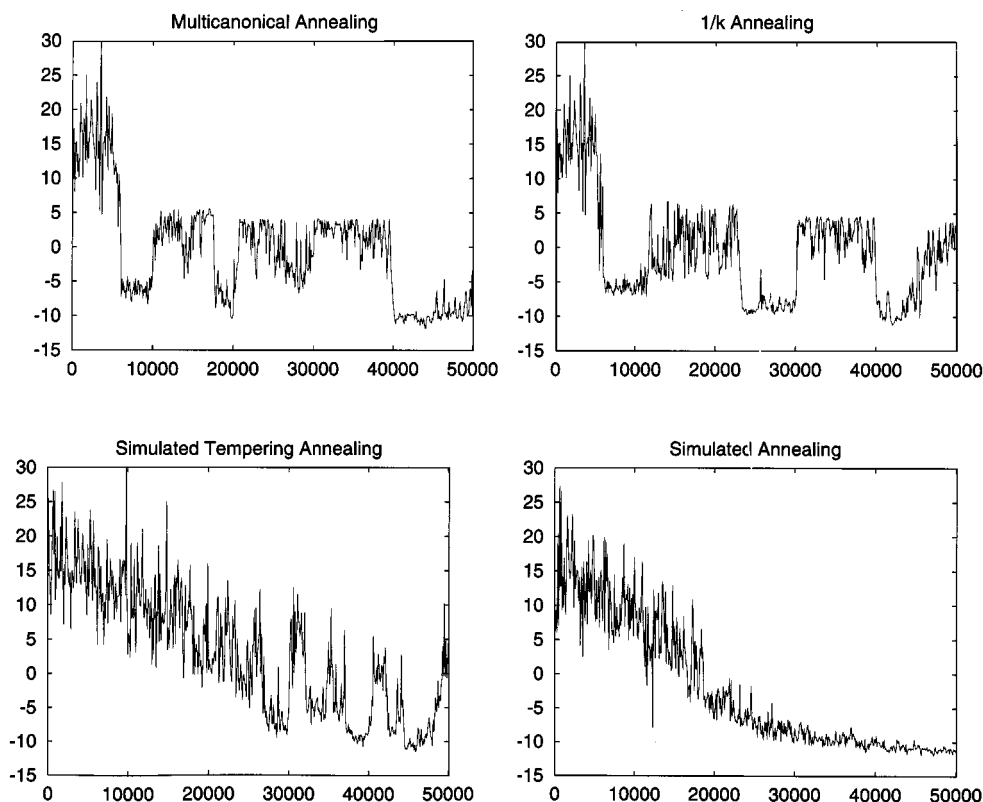


**FIGURE 6.** Time series of energy,  $E$  (kcal / mol), from an annealing simulation of 50,000 MC sweeps by multicanonical,  $1/k$ -sampling, simulated tempering, and simulated annealing algorithms.

Namely, as the simulation proceeds, the size of energy fluctuations is fixed to a preset finite value for the former three methods, whereas it decreases toward zero for the latter. Hence, the chance of getting trapped in an energy local minima becomes higher and higher as the simulation proceeds for Monte Carlo simulated annealing.

## Conclusions

We have performed simulations with high statistics for a simple peptide, met-enkephalin, to compare numerically the performances of three new algorithms in the protein folding problem. All three methods have in common that simulations are performed in a generalized ensemble instead of the usual canonical ensemble. They all require, as a first step, the calculation of estimators for the probability weight factors not *a priori* known. Using an analytical transformation of the obtained distribution to a canonical distribution, any thermodynamic quantity at any temperature can in

principle be calculated from one simulation run. We demonstrated that the calculated thermodynamic quantities over a wide range of temperatures were identical for the three methods. In particular, the agreement persisted into the difficult, low temperature regime, where regular canonical simulations will necessarily get trapped in one of many energy local minima. Hence, one can cross-check the low temperature results obtained from one of the three methods by those of another. Furthermore, by comparing the efficiency of the three methods in finding independent ground-state structures, we found that the three methods are equally more effective than traditional methods.

We conclude that all three methods are equally well suited for the simulation of peptides and proteins. Temperature, energy, or entropy are also by no means the only variables in which a uniform sampling is possible, nor is there any restriction on any one variable. The three studied algorithms are only special cases of a larger class of similar methods, which we may call simulations in the *generalized ensemble*.

## Acknowledgments

Our simulations were performed on a cluster of fast RISC workstations at SCRI (Florida State University, Tallahassee, FL) and computers at the Computer Center of the Institute for Molecular Science (IMS), Okazaki, Japan. Part of this work was done while one of us (U.H.) was a visitor at the IMS. U.H. thanks the members of the IMS for the kind hospitality extended to him.

## References

1. M. Vásquez, G. Némethy, and H. A. Scheraga, *Chem. Rev.*, **94**, 2183 (1994).
2. Z. Li and H. A. Scheraga, *Proc. Nat. Acad. Sci. USA*, **84**, 6611 (1987).
3. R. S. Judson, M. E. Colvin, J. C. Meza, A. Huffer, and D. Gutierrez, *Int. J. Quantum Chem.*, **44**, 277 (1992); T. Dandekar and P. Argos, *Prot. Eng.*, **5**, 637 (1992).
4. S. Kirkpatrick, C. D. Gelatt, Jr., and M. P. Vecchi, *Science*, **220**, 671 (1983).
5. M. Nilges, A. M. Gronenborn, A. T. Brünger, and G. M. Clore, *Prot. Eng.*, **2**, 27 (1988).
6. S. R. Wilson, W. Cui, J. W. Moskowicz, and K. E. Schmidt, *Tetrahed. Lett.*, **29**, 4373 (1988).
7. H. Kawai, T. Kikuchi, and Y. Okamoto, *Prot. Eng.*, **3**, 85 (1989).
8. C. Wilson and S. Doniach, *Proteins*, **6**, 193 (1989).
9. S. R. Wilson and W. Cui, in *The Protein Folding Problem and Tertiary Structure Prediction*, K. M. Merz, Jr. and S. M. Legrand, Eds., Birkhäuser, Berlin, 1994, p. 43.
10. B. A. Berg and T. Neuhaus, *Phys. Lett.*, **B267**, 249 (1991); *Phys. Rev. Lett.*, **68**, 9 (1992).
11. B. A. Berg, *Int. J. Mod. Phys.*, **C3**, 1083 (1992).
12. J. Lee, *Phys. Rev. Lett.*, **71**, 211 (1993); *Phys. Rev. Lett.*, **71**, 2353(E) (1993).
13. A. P. Lyubartsev, A. A. Martinovski, S. V. Shevkunov, and P. N. Vorontsov-Velyaminov, *J. Chem. Phys.*, **96**, 1776 (1992).
14. E. Marinari and G. Parisi, *Europhys. Lett.*, **19**, 451 (1992).
15. B. Hesselbo and R. B. Stinchcombe, *Phys. Rev. Lett.*, **74**, 2151 (1995).
16. B. A. Berg, U. H. E. Hansmann, and Y. Okamoto, *J. Phys. Chem.*, **99**, 2236 (1995); but see also the reply by M. H. Hao and H. A. Scheraga, *J. Phys. Chem.*, **99**, 2238 (1995).
17. U. H. E. Hansmann and Y. Okamoto, *J. Comput. Chem.*, **14**, 1333 (1993).
18. U. H. E. Hansmann and Y. Okamoto, *J. Phys. Soc. Jpn.*, **63**, 3945 (1994); *Physica A*, **212**, 415 (1994).
19. M. H. Hao and H. A. Scheraga, *J. Phys. Chem.*, **98**, 4940 (1994).
20. Y. Okamoto, U. H. E. Hansmann, and T. Nakazawa, *Chem. Lett.*, 391 (1995); Y. Okamoto and U. H. E. Hansmann, *J. Phys. Chem.*, **99**, 11276 (1995).
21. A. Irbäck and F. Potthast, *J. Chem. Phys.*, **103**, 10298 (1995).
22. R. H. Swendsen and J. S. Wang, *Phys. Rev. Lett.*, **58**, 86 (1987).
23. R. G. Edwards and A. Sokal, *Phys. Rev.*, **D38**, 2009 (1988).
24. A. M. Ferrenberg and R. H. Swendsen, *Phys. Rev. Lett.*, **61**, 2635 (1988); *Phys. Rev. Lett.*, **63**, 1658(E) (1989), and references given in the erratum.
25. N. Metropolis, A. W. Rosenbluth, M. N. Rosenbluth, A. H. Teller, and E. Teller, *J. Chem. Phys.*, **21**, 1087 (1953).
26. B. von Freyberg and W. Braun, *J. Comput. Chem.*, **12**, 1065 (1991).
27. Y. Okamoto, T. Kikuchi, and H. Kawai, *Chem. Lett.*, 1275, (1992).
28. F. A. Momany, R. F. McGuire, A. W. Burgess, and H. A. Scheraga, *J. Phys. Chem.*, **79**, 2361 (1975).
29. G. Némethy, M. S. Pottle, and H. A. Scheraga, *J. Phys. Chem.*, **87**, 1883 (1983).
30. M. J. Sipple, G. Némethy, and H. A. Scheraga, *J. Phys. chem.*, **88**, 6231 (1984).
31. H. Kawai, Y. Okamoto, M. Fukugita, T. Nakazawa, and T. Kikuchi, *Chem. Lett.*, 213 (1991); Y. Okamoto, M. Fukugita, T. Nakazawa, and H. Kawai, *Prot. Eng.*, **4**, 639 (1991).
32. J. Lee and M. Y. Choi, *Phys. Rev.*, **E50**, R651 (1994).